JOURNAL OF BACTERIOLOGY, Jan. 2000, p. 164–170 Vol. 182, No. 1
0021-9193/00/$04.00+0

Straight and Curved Conformations of FtsZ Are Regulated by GTP Hydrolysis

CHUNLIN LU, MARY REEDY, AND HAROLD P. ERICKSON*

Department of Cell Biology, Duke University Medical Center, Durham, North Carolina 27710

Received 31 March 1999/Accepted 4 October 1999

FtsZ assembles in vitro into protofilaments that can adopt two conformations—the straight conformation, which can assemble further into two-dimensional protofilament sheets, and the curved conformation, which forms minirings about 23 nm in diameter. Here, we describe the structure of FtsZ tubes, which are a variation of the curved conformation. In the tube the curved protofilament forms a shallow helix with a diameter of 23 nm and a pitch of 18 or 24°. We suggest that this shallow helix is the relaxed structure of the curved protofilament in solution. We provide evidence that GTP favors the straight conformation while GDP favors the curved conformation. In particular, exclusively straight protofilaments and protofilament sheets are assembled in GMPCPP, a nonhydrolyzable GTP analog, or in GTP following chelation of Mg, which blocks GTP hydrolysis. Assembly in GDP produces exclusively tubes. The transition from straight protofilaments to the curved conformation may provide a mechanism whereby the energy of GTP hydrolysis is used to generate force for the constriction of the FtsZ ring in cell division.

FtsZ is a major cytoskeletal protein in all bacteria and archaea, where it forms the framework for the cell-division machinery at the site of septation (3, 9, 17). Light microscopy shows FtsZ localized in a ring at the site of septation, apparently just under the cell membrane; the ring constricts as septation proceeds (1, 14, 18). The role of FtsZ as a structural protein is indicated by its abundance (15,000 molecules per average *Escherichia coli* cell [6, 16]) and its assembly into protofilaments in vitro (11, 16, 20, 21, 27). In addition to providing the structural framework for the division apparatus, we suggest that FtsZ may also generate the force that powers constriction of the FtsZ ring. A possible mechanism for generating force is the transition of the protofilament from the straight to the curved conformation (reference 9; also see Discussion).

The structure of FtsZ polymers in bacteria has never been visualized, but much has been learned from polymers assembled in vitro. These in vitro polymers show the range of structures that are possible, providing insight into potential in vivo structures. Four polymer forms assembled by *E. coli* FtsZ are shown in Fig. 1. Single, straight protofilaments (16, 21), sheets of straight protofilaments (11, 27), and minirings (11) have been described previously. Tubular polymers of FtsZ have also been reported (4, 8, 20, 25), but their substructure has not been determined previously. Here, we describe the structure of FtsZ tubes and demonstrate that they are a variation of the curved protofilament conformation. We then investigate how GTP and GDP favor the straight and curved conformations, respectively.

MATERIALS AND METHODS

The nonhydrolyzable GTP analog GMPCPP was generously provided by John J. Correia, University of Mississippi Medical Center, Jackson, Miss. Other reagents were purchased from Sigma (St. Louis, Mo.) or as noted below.

Purification of FtsZ. Wild-type FtsZ was expressed in *E. coli* and purified by a two-step ammonium sulfate precipitation, as described previously (16). Briefly, the bacterial cell lysate was centrifuged, the supernatant was brought to 20% saturated ammonium sulfate, and the precipitated protein, mostly inactive FtsZ, was discarded. The active FtsZ was then precipitated by increasing the ammonium sulfate to 25% saturation. Buffers were exchanged by dialysis or by small gel filtration columns. Protein concentration was determined by our calibrated bicinchoninic acid assay (Pierce, Rockford, Ill.), using bovine serum albumin as a standard and correcting for the 0.75 ratio of color produced by FtsZ relative to bovine serum albumin (16).

Assembly and electron microscopy. Assembly of FtsZ in vitro was routinely carried out in 30 μl of MEMK6.5 buffer (100 mM morpholineethanesulfonic acid, pH 6.5, adjusted with KOH–1 mM EGTA–5 mM Mg acetate) containing 1 mg of FtsZ per ml, 2 mM GTP or 2 mM GDP, and variable concentrations of DEAE-dextran. The reaction mixture was incubated on ice for 5 to 10 min and then at 37°C for 5 to 10 min, and negatively stained electron microscope specimens were prepared. Reaction mixture (10 μl) was applied to a carbon-coated grid and washed off with 2% aqueous uranyl acetate. Electron micrographs were taken at a magnification of ×50,000.

To quantitate assembly of FtsZ with DEAE-dextran, samples were centrifuged at 20,000 × *g* for 15 min, and the FtsZ protein in the pellet was determined by the bicinchoninic acid assay.

To prepare samples for cross-sectioning, FtsZ was assembled in a 200-μl volume as described above. After 5 min of incubation at 37°C, glutaraldehyde (ultrapure transmission electron microscopy grade; Tousimis Research Corporation, Rockville, Md.) was added to a concentration of 1%, and then the mixture was incubated for another 2 min at 37°C. Polymers were collected by centrifuging at 20,000 × *g* at room temperature for 10 min. Pellets were further fixed with 3% glutaraldehyde and 0.2% tannic acid (Electron Microscopy Sciences, Fort Washington, Pa.), postfixed in OsO_4, block stained with uranyl acetate, dehydrated in ethanol, and embedded in Araldite 506 (Tousimis). Silver and grey sections were stained first with $KMnO_4$ in H_2O and then with Sato lead (24).

RESULTS

Four types of polymers formed by FtsZ. We found and confirmed that FtsZ assembled into the four types of polymers shown in Fig. 1. FtsZ protofilaments (Fig. 1a) formed spontaneously in several buffers and at pH values ranging from 6 to 8; assembly of these straight protofilaments required GTP (16, 21). These protofilaments of pure FtsZ sometimes associated into bundles or sheets (see Fig. 1d of reference 11). Assembly of sheets (Fig. 1b) was highly stabilized and favored by addition of the polycation DEAE-dextran (11) or Ca (reference 27 and results discussed below). Minirings (Fig. 1c), which were identified as protofilaments in a curved conformation, were found when FtsZ was assembled onto a cationic lipid monolayer (11). Tubular polymers (Fig. 1d) have been reported previously (4,

* Corresponding author. Mailing address: Department of Cell Biology, 3011, Duke University Medical Center, Durham, NC 27710. Phone: (919) 684-6385. Fax: (919) 684-3687. E-mail: H.Erickson@cellbio.duke.edu.

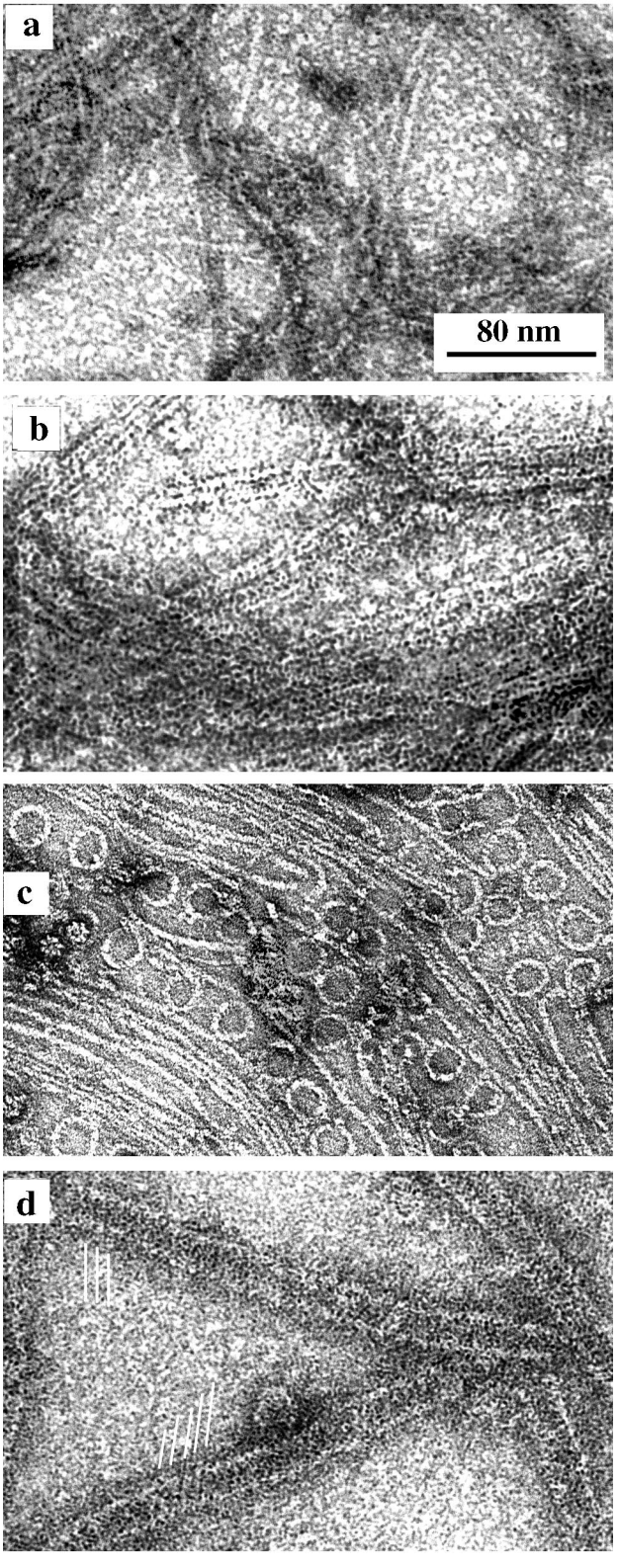

FIG. 1. The four types of polymers formed by FtsZ in MEMK6.5. (a) Straight protofilaments formed with GTP but without DEAE-dextran; (b) sheets of straight protofilaments assembled from FtsZ plus DEAE-dextran; (c) minirings assembled with GDP and adsorbed onto a cationic lipid monolayer; (d) FtsZ tubes assembled with GDP and DEAE-dextran. The parallel white lines indicate the helical protofilaments in these tubes.

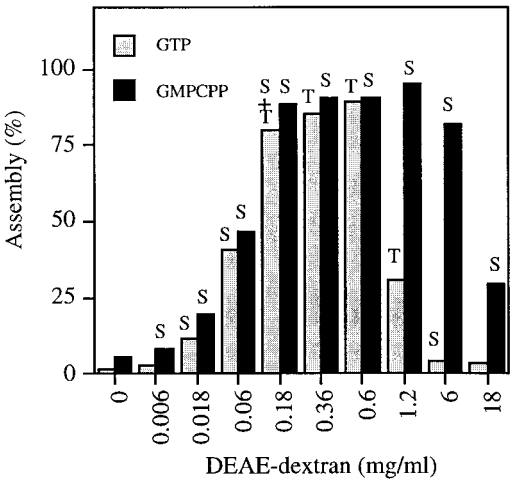

FIG. 2. Total polymer formed with varying amounts of DEAE-dextran. All samples contained 1 mg of FtsZ per ml and either 2 mM GTP or 2 mM GMPCPP. The polymer forms seen by electron microscopy after 10 min of assembly are indicated above the bars. S, sheets; T, tubes. Note that single straight protofilaments are formed in the absence of DEAE-dextran, but these are not pelleted in the 20,000 × *g* centrifugation used in this assay. Assembly in GTP plus EDTA yielded a profile identical to that for assembly in GMPCPP.

8, 20, 25); here, we have determined the optimal conditions for their assembly and their structure.

Quantitative assay of assembly of FtsZ plus DEAE-dextran. In a previous study, members of our group used a medium-speed centrifugation (20,000 × *g*) to quantitate the FtsZ polymers assembled with DEAE-dextran. This centrifugation was sufficient to pellet both sheets and tubes but not individual protofilaments. At 1 mg of FtsZ per ml, we found a peak of assembly at 0.6 mg of DEAE-dextran per ml (16), while the amount of DEAE-dextran–FtsZ complex was substantially reduced at levels of DEAE-dextran that were 10-fold higher or lower. Results from a similar experiment are shown in Fig. 2, with additional observations. We have found that a DEAE-dextran-to-FtsZ weight ratio of 0.6:1 yields maximum assembly of the large polymers over a range of FtsZ concentrations. Trusca et al. (25) found a peak assembly at about the same ratio.

Electron microscopy showed a striking change in polymer form at the different ratios of DEAE-dextran to FtsZ. At 0.06 and 6 mg of DEAE-dextran per ml, the polymers were all protofilament sheets, but at a concentration of 0.6 mg/ml, which yields the peak level of assembly, they were almost all tubes. These observations were made 10 min after assembly was initiated by adding DEAE-dextran to the mixture of FtsZ plus GTP. The 0.6-mg/ml DEAE-dextran sample showed some sheets at 1 min, and we believe that the tubes represent a transition following GTP hydrolysis (see Discussion). A different polymerization profile was obtained with the nonhydrolyzable analog GMPCPP (Fig. 2) and is addressed below.

Thin section electron microscopy of sheets and tubes. To confirm the structure of the sheets and tubes previously visualized in negative stain, we examined the polymers by embedding and sectioning. The thin sections (Fig. 3) provided two new perspectives. First, they confirmed that the polymer pelleted after fixation was exclusively sheets or tubes and did not contain amorphous aggregates, which may have been missed in the negative stain. Second, they provided views of the polymers in cross-section. This was particularly important for the sheets, which revealed a surprising two-layer structure. Assembly in

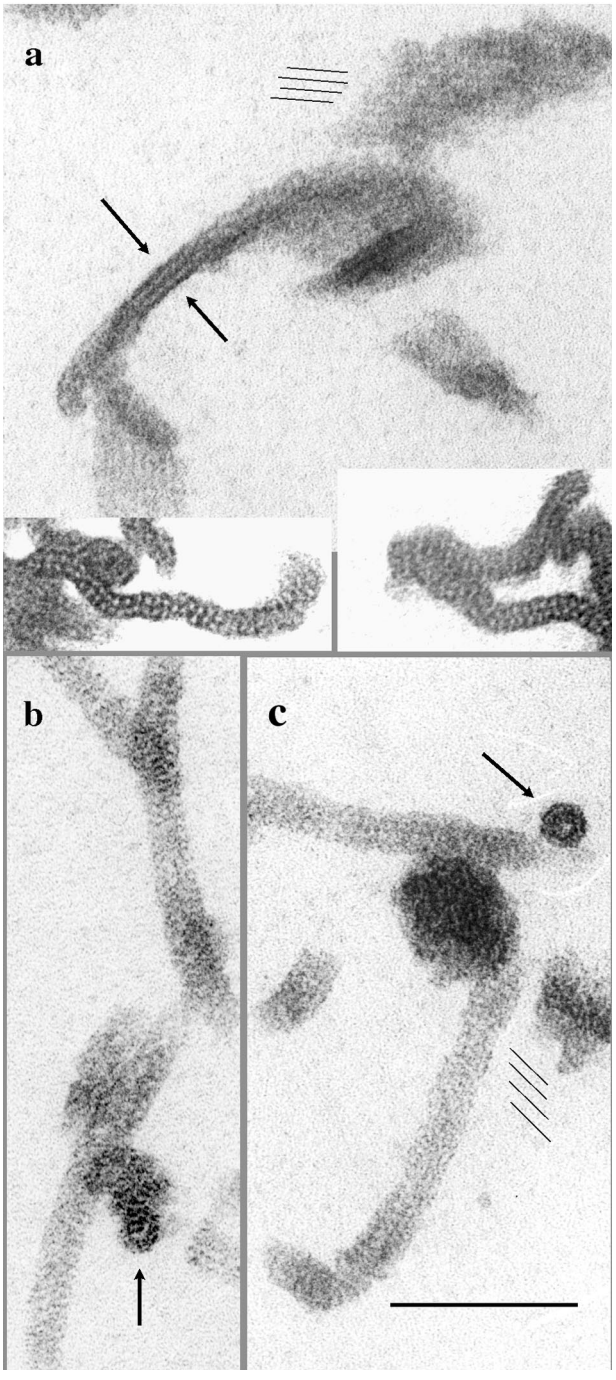

FIG. 3. Thin sections of FtsZ polymers. (a) Sheets assembled with 0.6 mg of DEAE-dextran per ml plus 2 mM GTP plus 10 mM EDTA. The thinnest profiles show a trilaminar structure, ~12 nm thick, and are probably two sheets face-to-face (arrows). Face views of the sheets show the protofilament structure (parallel thin lines). The insets show cross-sections where individual protofilaments are resolved as two slightly offset rows. (b and c) Tubes assembled with 0.6 mg of DEAE-dextran per ml plus GTP, allowing 10 min for hydrolysis and tube formation. The arrows indicate tubes in cross-section. Longitudinal sections of tubes sometimes show striations due to the helical protofilaments (parallel thin lines). Bar, 100 nm.

GTP plus EDTA yielded the largest and best-defined sheets, and these had a distinct 12-nm-thick, trilaminar profile in cross-section (Fig. 3a). We interpreted these to be two sheets face-to-face (if they were face-to-back, larger stacks should also have been formed). The three dark lines of the cross-section correspond to stain coating the protein surfaces on the outside and the interface between the two sheets. In some cross-sections individual protofilaments were resolved, and these were clearly arranged in two, somewhat irregular layers (Fig. 3a, insets). Sheets that formed in lower concentrations of DEAE-dextran without EDTA also showed mostly trilaminar profiles, implying that most of the sheets in these preparations were two-layer. The sheets used for computer reconstruction in a previous study (11) appeared to be single layers, but these have been difficult to reproduce in the present assembly conditions. The thin sections of tubes showed the expected profiles of cylinders in longitudinal and cross-sectional views (Fig. 3b).

Structure of FtsZ tubes—curved protofilaments with a helical displacement. Previous studies have shown that FtsZ plus DEAE-dextran can assemble into tubular polymers (8, 20, 25). Similar polymers have been obtained at low pH values in the absence of DEAE-dextran (4). We have determined that tubes can be reproducibly assembled from 1 mg of FtsZ per ml plus 0.6 mg of DEAE-dextran per ml in the presence of either GTP or GDP (Fig. 4). The outside diameter of the tubes was measured to be 23 ± 2.1 nm (average ± standard deviation, n = 35), the same diameter as FtsZ minirings (11).

These tubes are quite different from microtubules, which show prominent straight protofilaments parallel to the axis of the tube. FtsZ tubes never show longitudinal protofilaments, but they frequently show oblique striations (Fig. 1 and 3). The nature of these striations is revealed most clearly in partially assembled tubes, which we have found in some specimens. The partial tubes shown in Fig. 4a and b appear to be spirals of two protofilaments forming a shallow helix. Between the gyres of this helix is a space about the same thickness as the double protofilament. In some places the space is filled in to produce a more solid tube (Fig. 4b and 4c).

There are two possibilities for the transition from the open, helical gyres to the more compact, solid tubes. One is that the helix of the open gyres could simply collapse to a smaller pitch. Trusca et al. (25) recently presented images of FtsZ tubes that are essentially identical to ours, showing some tubes with a pair of helical protofilaments like those shown in Fig. 4a and b, and some solid tubes like that shown in Fig. 4c. They suggested the collapse hypothesis. The second possibility is that the space between the two helical protofilaments is filled in by two more protofilaments, each with the same pitch as the original helix. We now provide evidence from optical diffraction that supports this second hypothesis.

Images of intact tubes were surveyed for highly ordered segments that gave good optical diffraction patterns; an example is shown in the inset of Fig. 4c. The pattern shows two horizontal streaks on layer lines above and below the equator. The spacing of the layer lines from the equator indicates that adjacent protofilaments are 5.4 nm apart, about the same as the 5.3-nm spacing of straight protofilaments in the sheets (11). The angle of the spots from the vertical indicates the pitch of the helices. About half of the tubes showed an angle of 18°, and the rest showed an angle of 24°. With 16 subunits per turn spaced 4.3 nm apart, the 18° pitch would mean that the protofilament rises 21 nm per turn, which is four times the 5.4-nm spacing between adjacent protofilaments. This means that four helices are required to make the solid tube with the 18° pitch, and five helices are required for the 24° pitch. The pitch of these solid tubes is approximately the same as that of the open, two-protofilament helices in Fig. 4a and b, indicating that the solid tubes are formed by filling in the spaces with an additional two or three helices, rather than collapsing the two

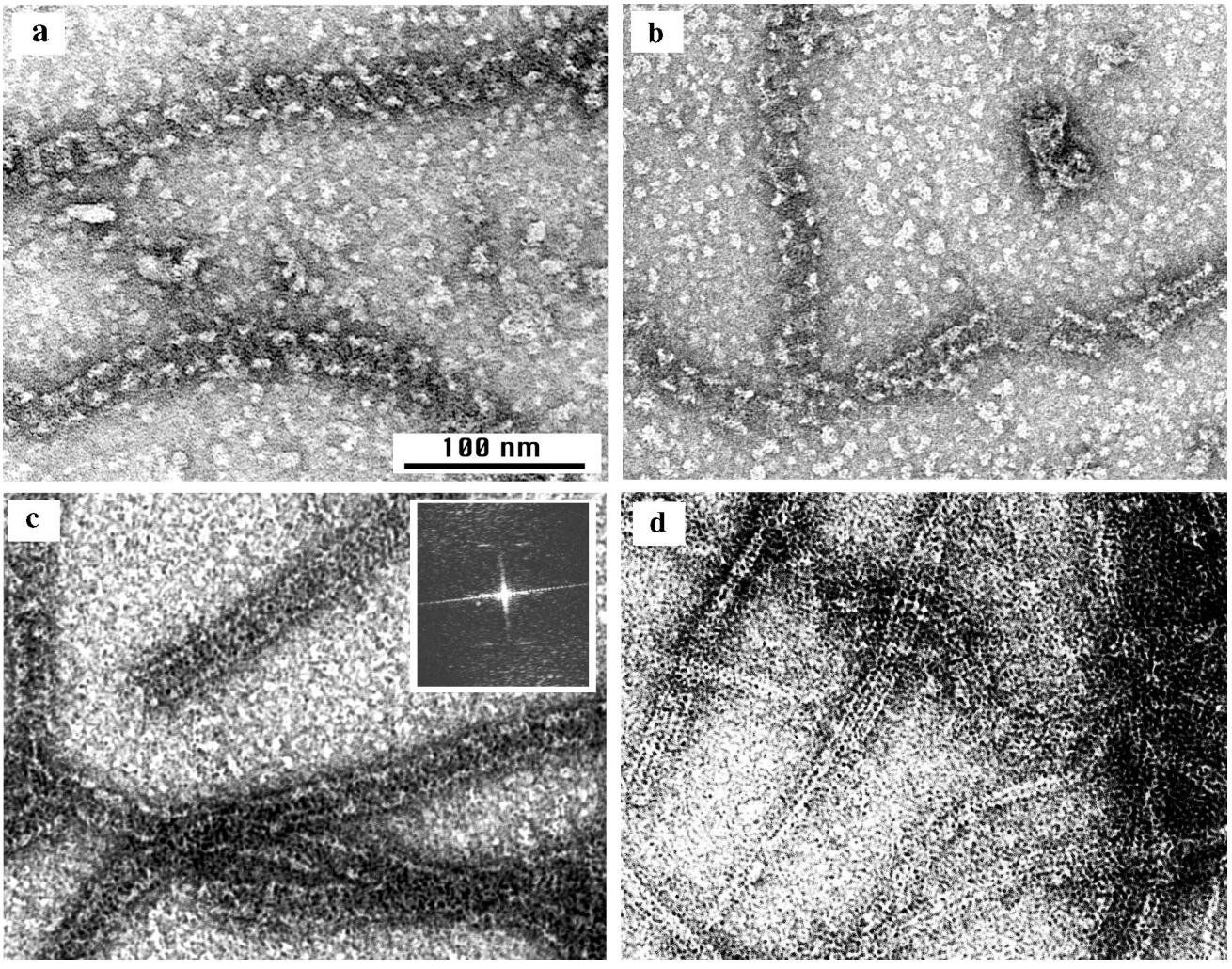

FIG. 4. FtsZ tubular polymers. (a and b) Two examples of partial tubes showing the helical substructure. These samples were fixed with glutaraldehyde after a 10-min assembly of FtsZ, DEAE-dextran, and GDP at 37°C prior to negative staining. They appear to be spirals of two protofilaments, with a gap approximately the same width as the protofilament pair. The tube at the right of panel b has filled in the gap. (c) Intact tubes negatively stained. The helical protofilaments from the top and bottom surfaces superimpose to form a complex pattern. The inset shows an optical diffraction pattern of one of these tubes. (d) When 10 mM GTP, or 2 mM GTP plus 10 mM EDTA, was added to a preparation of tubes, they showed a very rapid transition to sheets. Many of these sheets had four protofilaments.

helices to a smaller pitch. The deduced structure of the tubes is shown in Fig. 5.

Additional evidence for the four-start helix was obtained in an experiment generating an abrupt transformation of tubes to sheets. A sample of tubes was prepared from a solution containing 1 mg of FtsZ per ml, 0.6 mg of DEAE-dextran per ml, and 2 mM GDP and applied to an electron microscope grid. The grid was washed first with a drop of assembly buffer containing 10 mM GTP (which simultaneously chelates the Mg and supplies external GTP; both are important for the transition [15]) and immediately after with uranyl acetate. Most of the tubes had transformed completely into sheets in the ~15 seconds in GTP, and most of the sheets had four protofilaments (Fig. 4d). If a paper model of the four-start helix is cut in a spiral between any one pair of protofilaments and then straightened, a four-protofilament sheet is produced. The prominence of four-protofilament sheets is consistent with a direct straightening of the four-start helix.

In our previous study (11), we observed curved protofilaments forming minirings in specimens adsorbed to polycationic lipid monolayers. We have searched extensively for minirings in solution but have never found them. Instead, in the GDP assembly where we expected to find minirings, we found tubes. We now believe that the miniring is a distorted form of the curved protofilament, produced when the curved protofilament binds to a lipid monolayer. Because the monolayer is planar the curved protofilament is constrained to a flat circle. When the curved protofilament is free in solution, however, its natural form is not a flat circle, but a shallow helix.

In summary, three lines of evidence support the conclusion that the curved conformation of the relaxed protofilament is a shallow helix, 23 nm in diameter and with a pitch of 18 or 24°. First, the tubes and minirings have the same 23-nm diameter. Second, the 18 or 24° pitch is seen for the unconstrained pairs of protofilaments in the incomplete tubes (Fig. 4a and b). Third, the same pitch is demonstrated for the intact tube by optical diffraction (Fig. 4c). We should note also that the structure of the tube as a hollow cylinder is confirmed in thin section (Fig. 3b). The structure of the tubes compared to rings and straight protofilaments is shown diagrammatically in Fig. 5.

Calcium can stabilize polymers similar to DEAE-dextran. Yu and Margolin (27) reported that Ca can stabilize the as-

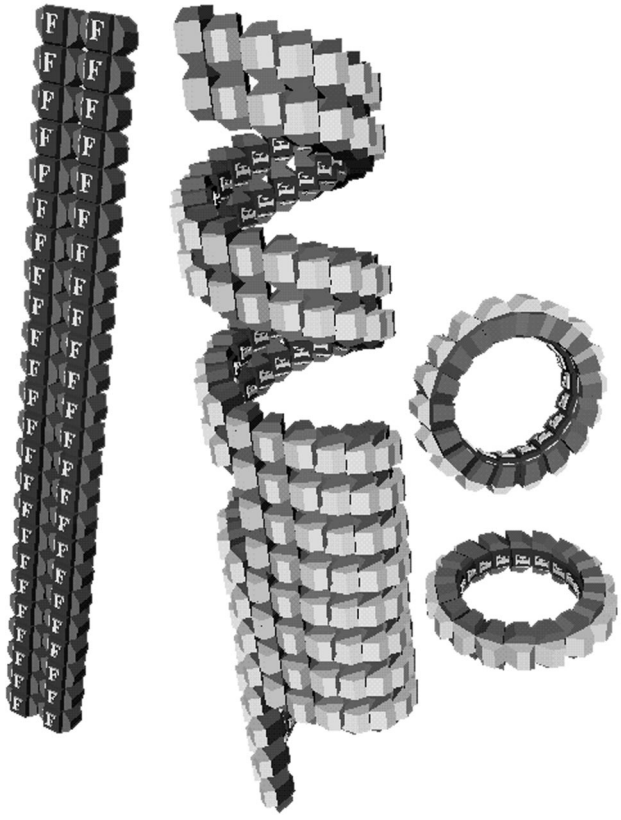

FIG. 5. Model of the FtsZ tube. The top section is a partial tube, comprising a pair of helical protofilaments with a space between them about equal to the width of the pair. The bottom section is a solid tube, where two additional protofilaments have filled this space. For comparison, a pair of straight protofilaments is indicated on the left, and two minirings are shown on the right. We suggest that the helical protofilament is the relaxed form of the curved conformation and that minirings are formed only when the curved protofilaments are bound to a planar lipid monolayer.

sembly of protofilament sheets or bundles, so we wanted to compare these Ca polymers to those assembled in DEAE-dextran. At Ca concentrations below 5 mM, FtsZ assembled into protofilaments similar to those formed without Ca or DEAE-dextran. When the Ca concentration was increased to 10 or 20 mM the protofilaments associated into sheets or bundles (Fig. 6a), which were mostly narrower and less regular than those assembled in DEAE-dextran. Protofilament pairs seemed especially favored (Fig. 6b). Longitudinal thin sections were also consistent with a parallel bundle of protofilaments (Fig. 6c). In cross-sections these bundles mostly appeared thicker than a single sheet and had an irregular structure (Fig. 6d). The lateral packing of protofilaments in the calcium-stabilized bundles was less regular than that in the DEAE-dextran-stabilized sheets, which may indicate switching between two or more types of lateral contacts.

We were unable to obtain significant assembly in calcium plus GDP. A few tubular polymers could be detected by electron microscopy, but only a very small fraction of the FtsZ could be pelleted by centrifugation. However, we found convincing tubes and helical polymers in some specimens assembled in GTP. The two-protofilament helices shown in Fig. 6b appear to be identical to those assembled in DEAE-dextran (Fig. 4a and b). We conclude that the tubular polymers can exist in calcium-stabilized assembly but that they are less stable than those in DEAE-dextran. We believe that the helical polymers shown in Fig. 6b were initially formed as pairs of straight protofilaments, which transformed into the curved conformation as they hydrolyzed the GTP. The helical protofilaments in calcium seem to exist only transiently before depolymerizing.

GDP favors curved protofilaments (tubes), and GTP favors straight protofilaments. Previous studies have reported that FtsZ polymers stabilized by DEAE-dextran can be obtained with either GTP or GDP (11, 20), and we have confirmed that here. However, we have made the further observation that assembly of FtsZ plus DEAE-dextran in GDP produces only tubes (Fig. 1d, 3b, and 4). We therefore conclude that the preferred conformation for FtsZ-GDP polymer is the curved protofilament.

It was more difficult to determine the conformation preferred by FtsZ-GTP, because the nucleotide is hydrolyzed at an unknown rate in the polymer. Also, as explained above, we found that the polymer form changed depending on the ratio of DEAE-dextran to FtsZ and the time of assembly.

A nonhydrolyzable GTP analog might lock the polymer into the GTP conformation and provide a way to determine this. We initially tried GTPγS, which is known in many circumstances to be hydrolyzed slowly or not at all. However, we found that it gave assembly that was very similar to that in GTP. In particular, at the DEAE-dextran-to-FtsZ weight ratio of 0.6 the assembly gave predominantly tubes at 10 min. This suggests that the GTPγS is being hydrolyzed by FtsZ and is probably not a useful GTP analog.

GMPCPP has been used extensively for studies of tubulin assembly (5, 12, 13, 26), where it is hydrolyzed very slowly or not at all in most conditions. (There is one notable exception:

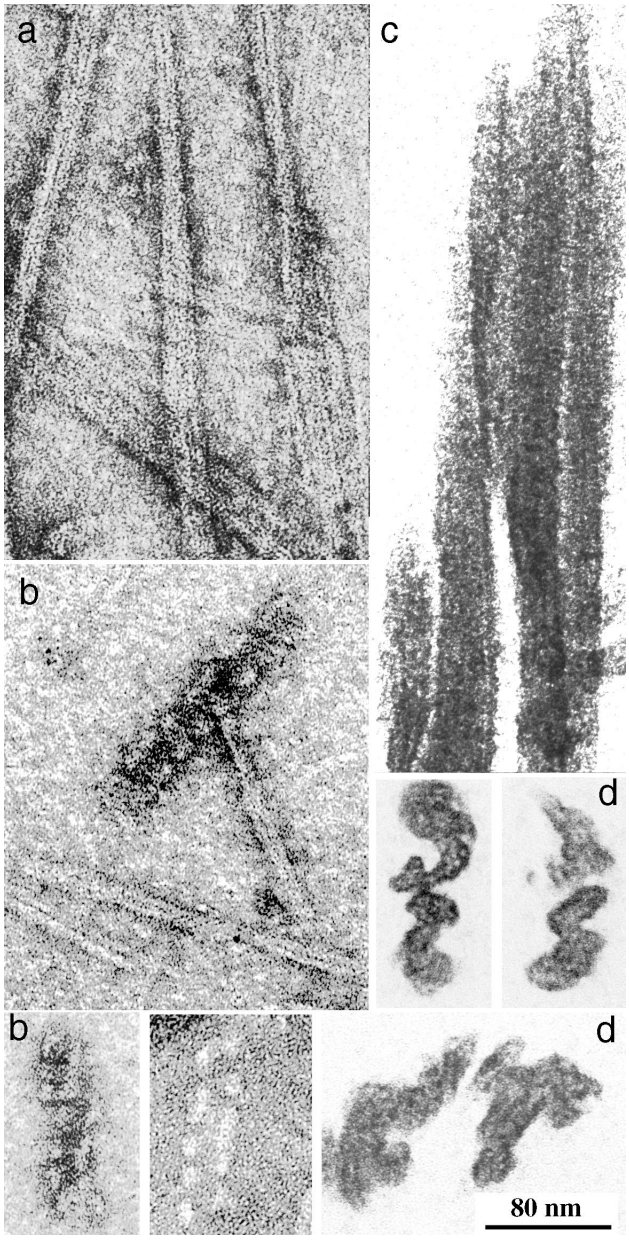

FIG. 6. Assembly of FtsZ in calcium. (a) Protofilament pairs, sheets, and bundles assembled in 20 mM $CaCl_2$–2 mM GTP for 10 min; (b) the same sample showed some short, two-protofilament helical spirals (similar to those shown in Fig. 4a and b) along with straight protofilament pairs. Images shown in panels a and b were negatively stained. (c and d) Longitudinal and cross-sectional profiles, respectively, of calcium polymers embedded and sectioned. The cross-sections show that the Ca-FtsZ polymers are thicker and less regular than the protofilament sheets stabilized by DEAE-dextran (cf. Fig. 3a).

in buffers containing 80 mM Na plus high concentrations of glycerol or glutamate, microtubules hydrolyze GMPCPP to GMPCP [5]. We did not use Na, glycerol, or glutamate in our buffers for the present study.) In the presence of 1 to 2 mM GMPCPP and in the absence of DEAE-dextran, FtsZ assembled into individual straight protofilaments, identical to those in GTP. When assembly was stimulated by increasing concentrations of DEAE-dextran and assayed by centrifugation, the profile for GMPCPP was different from that for GTP. In particular, the peak of maximal polymer now extended to much higher concentrations of DEAE-dextran (Fig. 2). However, the most striking change was in the morphology of the polymers. Whereas assembly in GTP produced tubes at the DEAE-dextran-to-FtsZ weight ratio of 0.6, assembly in GMPCPP produced sheets of straight protofilaments at all concentrations of DEAE-dextran. Tubes were never formed from FtsZ-GMPCPP.

We discovered that chelating the Mg provided an alternative way to trap the polymer in the GTP conformation. Mg is essential for GTP hydrolysis (7, 19, 23), but we have found that it is not necessary for assembly. Mukherjee and Lutkenhaus (22) have also recently reported assembly of protofilaments in the presence of EDTA. Assembly in GTP plus EDTA was identical in all respects to assembly in GMPCPP. In the absence of DEAE-dextran, assembly produced individual straight protofilaments. When assayed for large polymers by centrifugation at increasing concentrations of DEAE-dextran, assembly in GTP plus 10 mM EDTA gave exactly the same profile as that shown in Fig. 2 for GMPCPP. Finally, electron microscopy showed that polymers assembled from FtsZ-GTP in 10 mM EDTA were exclusively sheets at all DEAE-dextran concentrations, identical to the pattern of assembly with GMPCPP. Our interpretation is that EDTA chelates Mg and blocks GTP hydrolysis, locking the polymer in the GTP form.

DISCUSSION

The existence of the straight and curved conformations for FtsZ protofilaments has been established previously (11). The present study provides evidence that the relaxed form of the curved protofilament is not the planar circle formed on lipid monolayers, but a shallow helix. The tubes that we assemble in vitro are probably not formed in vivo, since they have never been seen in bacteria by electron microscopy. However, the curvature and helical pitch of individual protofilaments are likely important for the function of FtsZ. The 18° helical pitch amounts to an axial displacement of $5.4 \times 4 = 21.6$ nm after one complete turn, which means that a curved protofilament may be displaced by this amount after encircling a bacterium. This may explain the tendency of FtsZ to form arcs and spirals in cells (2, 18) and suggests that the mutant FtsZ26, which forms exaggerated spirals (2), might have an altered pitch.

The second major point of our study is that GTP favors the straight protofilament, while GDP favors the curved protofilament. These end points are quite clear, but the transitions are not yet obvious. The simplest model would propose that FtsZ-GTP is required for the initial assembly, and this forms straight protofilaments. Assembly then induces hydrolysis (10), and the straight protofilaments transform into curved ones. Something like this may occur in vivo (see below) but we have not been able to observe such a transition in vitro (see reference 15 for more detailed description of some transitions in vitro). In particular, the polymers assembled in DEAE-dextran seem to be locked into either sheets of straight protofilaments or tubes, probably depending on relative rates of initial assembly and GTP hydrolysis. If GTP hydrolysis occurs rapidly relative to assembly, curved protofilaments that grow into tubes may form (e.g., at a DEAE-dextran-to-FtsZ weight ratio of 0.6). If assembly occurs rapidly, bundles of straight protofilaments may be locked together before significant GTP hydrolysis can occur (e.g., at a weight ratio of 0.6). This would be similar to the case of microtubules, whose wall of straight protofilaments is prevented from adopting the curved conformation by lateral contacts with other protofilaments (curvature can occur only when protofilaments are released at the ends).

The 15,000 molecules of FtsZ in an average *E. coli* cell (6,

16) are sufficient to make a protofilament 60 μm long, enough to encircle the bacterium 20 times. We estimated the concentration of FtsZ to be 440 μg/ml in the average *E. coli* cell (16), so most of this should be assembled given the critical concentration of 20 to 50 μg/ml estimated in vitro (16, 21, 22). It seems likely that a band of 10 to 20 FtsZ protofilaments provides the cytoskeletal framework for cell division. Since no motor molecules have been identified in bacterial genomes or in screens for division mutants, we have suggested that FtsZ may also provide the motile force for constriction. The transition from the straight to the curved conformation provides a potential mechanism (9).

Expanding on this hypothesis, we would postulate that FtsZ is initially assembled as straight protofilaments, nucleated from one or a few points on the inner cell membrane (2) and forming attachments to the membrane as they grow longer. Attachment of protofilaments to the 0.9-μm-diameter inner membrane would require only a slight distortion from the straight conformation. As GTP hydrolysis proceeds the protofilaments are induced toward the curved conformation. However, if the protofilaments remained attached to the membrane they would initially not be able to achieve the curved conformation. Nevertheless, the tendency to curve could generate a force in this direction (although the pathway of force production, as subunits change from a 0 to a 22.5° bend, may be complex). If the total force on the membrane increased as additional protofilaments were assembled, eventually the force of curvature could overcome the rigidity of the cell wall and initiate constriction.

As was suggested previously (9), such a minimal division machine may actually be used by mycoplasmas, which have none of the accessory division proteins (e.g., FtsA, FtsQ, and FtsW) identified in *E. coli*. That would suggest that the accessory proteins are involved in specialized control and regulation in the bacteria that have them. FtsZ provides the major cytoskeletal framework for the division machine, and it may also provide the force for constriction through the straight to curved conformational change.

REFERENCES

1. **Addinall, S. G., E. F. Bi, and J. Lutkenhaus.** 1996. FtsZ ring formation in *fts* mutants. J. Bacteriol. **178:**3877–3884.
2. **Addinall, S. G., and J. Lutkenhaus.** 1996. FtsZ-spirals and -arcs determine the shape of the invaginating septa in some mutants of *Escherichia coli*. Mol. Microbiol. **22:**231–237.
3. **Bramhill, D.** 1997. Bacterial cell division. Annu. Rev. Cell Dev. Biol. **13:** 395–424.
4. **Bramhill, D., and C. M. Thompson.** 1994. GTP-dependent polymerization of *Escherichia coli* FtsZ protein to form tubules. Proc. Natl. Acad. Sci. USA **91:**5813–5817.
5. **Caplow, M., R. L. Ruhlen, and J. Shanks.** 1994. The free energy for hydrolysis of a microtubule-bound nucleotide triphosphate is near zero: all of the free energy for hydrolysis is stored in the microtubule lattice. J. Cell Biol. **127:**779–788.
6. **Dai, K., and J. Lutkenhaus.** 1992. The proper ratio of FtsZ to FtsA is required for cell division to occur in *Escherichia coli*. J. Bacteriol. **174:**6145–6151.
7. **de Boer, P., R. Crossley, and L. Rothfield.** 1992. The essential bacterial cell division protein FtsZ is a GTPase. Nature **359:**254–256.
8. **Erickson, H. P.** 1995. FtsZ, a prokaryotic homolog of tubulin? Cell **80:**367–370.
9. **Erickson, H. P.** 1997. FtsZ, a tubulin homolog, in prokaryote cell division. Trends Cell Biol. **7:**362–367.
10. **Erickson, H. P.** 1998. Atomic structures of tubulin and FtsZ. Trends Cell Biol. **8:**133–137.
11. **Erickson, H. P., D. W. Taylor, K. A. Taylor, and D. Bramhill.** 1996. Bacterial cell division protein FtsZ assembles into protofilament sheets and minirings, structural homologs of tubulin polymers. Proc. Natl. Acad. Sci. USA **93:**519–523.
12. **Hyman, A. A., D. Chrétien, I. Arnal, and R. H. Wade.** 1995. Structural changes accompanying GTP hydrolysis in microtubules: information from a slowly hydrolyzable analogue, GMPCPP. J. Cell Biol. **128:**117–125.
13. **Hyman, A. A., S. Salser, D. N. Drechsel, N. Unwin, and T. J. Mitchison.** 1992. Role of GTP hydrolysis in microtubule dynamics: information from a slowly hydrolyzable analogue, GMPCPP. Mol. Biol. Cell **3:**1155–1167.
14. **Levin, P. A., and R. Losick.** 1996. Transcription factor Spo0A switches the localization of the cell division protein FtsZ from a medial to a bipolar pattern in *Bacillus subtilis*. Genes Dev. **10:**478–488.
15. **Lu, C., and H. P. Erickson.** The straight and curved conformation of FtsZ protofilaments—evidence for rapid exchange of GTP into the curved protofilament. Cell Struct. Funct., in press.
16. **Lu, C., J. Stricker, and H. P. Erickson.** 1998. FtsZ from *Escherichia coli*, *Azotobacter vinelandii*, and *Thermotoga maritima*—quantitation, GTP hydrolysis, and assembly. Cell Motil. Cytoskelet. **40:**71–86.
17. **Lutkenhaus, J., and S. G. Addinall.** 1997. Bacterial cell division and the Z ring. Annu. Rev. Biochem. **66:**93–116.
18. **Ma, X., D. W. Ehrhardt, and W. Margolin.** 1996. Colocalization of cell division proteins FtsZ and FtsA to cytoskeletal structures in living *Escherichia coli* cells by using green fluorescent protein. Proc. Natl. Acad. Sci. USA **93:**12998–13003.
19. **Mukherjee, A., K. Dai, and J. Lutkenhaus.** 1993. *Escherichia coli* cell division protein FtsZ is a guanine nucleotide binding protein. Proc. Natl. Acad. Sci. USA **90:**1053–1057.
20. **Mukherjee, A., and J. Lutkenhaus.** 1994. Guanine nucleotide-dependent assembly of FtsZ into filaments. J. Bacteriol. **176:**2754–2758.
21. **Mukherjee, A., and J. Lutkenhaus.** 1998. Dynamic assembly of FtsZ regulated by GTP hydrolysis. EMBO J. **17:**462–469.
22. **Mukherjee, A., and J. Lutkenhaus.** 1999. Analysis of FtsZ assembly by light scattering and determination of the role of divalent metal cations. J. Bacteriol. **181:**823–832.
23. **RayChaudhuri, D., and J. T. Park.** 1992. Escherichia coli cell-division gene *ftsZ* encodes a novel GTP-binding protein. Nature **359:**251–254.
24. **Reedy, M. K., and M. Reedy.** 1985. Rigor crossbridge structure in tilted single filament layers and flared-X formations from insect flight muscle. J. Mol. Biol. **185:**145–176.
25. **Trusca, D., S. Scott, C. Thompson, and D. Bramhill.** 1998. Bacterial SOS checkpoint protein SulA inhibits polymerization of purified FtsZ cell division protein. J. Bacteriol. **180:**3946–3953.
26. **Vulevic, B., and J. J. Correia.** 1997. Thermodynamic and structural analysis of microtubule assembly: the role of GTP hydrolysis. Biophys. J. **72:**1357–1375.
27. **Yu, X. C., and W. Margolin.** 1997. Ca^{2+}-mediated GTP-dependent dynamic assembly of bacterial cell division protein FtsZ into asters and polymer networks *in vitro*. EMBO J. **16:**5455–5463.